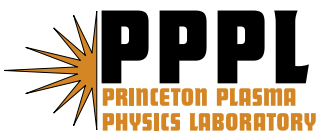

Princeton Plasma Physics Laboratory

PPPL-

PPPL-



Prepared for the U.S. Department of Energy under Contract DE-AC02-76CH03073.

Princeton Plasma Physics Laboratory

Report Disclaimers

Full Legal Disclaimer

This report was prepared as an account of work sponsored by an agency of the United States Government. Neither the United States Government nor any agency thereof, nor any of their employees, nor any of their contractors, subcontractors or their employees, makes any warranty, express or implied, or assumes any legal liability or responsibility for the accuracy, completeness, or any third party's use or the results of such use of any information, apparatus, product, or process disclosed, or represents that its use would not infringe privately owned rights. Reference herein to any specific commercial product, process, or service by trade name, trademark, manufacturer, or otherwise, does not necessarily constitute or imply its endorsement, recommendation, or favoring by the United States Government or any agency thereof or its contractors or subcontractors. The views and opinions of authors expressed herein do not necessarily state or reflect those of the United States Government or any agency thereof.

Trademark Disclaimer

Reference herein to any specific commercial product, process, or service by trade name, trademark, manufacturer, or otherwise, does not necessarily constitute or imply its endorsement, recommendation, or favoring by the United States Government or any agency thereof or its contractors or subcontractors.

PPPL Report Availability

Princeton Plasma Physics Laboratory:

<http://www.pppl.gov/techreports.cfm>

Office of Scientific and Technical Information (OSTI):

<http://www.osti.gov/bridge>

Related Links:

[U.S. Department of Energy](#)

[Office of Scientific and Technical Information](#)

[Fusion Links](#)

Accepted Manuscript

MARFE stability and movement in an ELM_y H-mode NSTX Discharge

F. Kelly, R. Maingi, R. Maqueda, J. Menard, S. Paul

PII: S0022-3115(09)00151-2

DOI: [10.1016/j.jnucmat.2009.01.122](https://doi.org/10.1016/j.jnucmat.2009.01.122)

Reference: NUMA 44197

To appear in: *Journal of Nuclear Materials*



Please cite this article as: F. Kelly, R. Maingi, R. Maqueda, J. Menard, S. Paul, MARFE stability and movement in an ELM_y H-mode NSTX Discharge, *Journal of Nuclear Materials* (2009), doi: [10.1016/j.jnucmat.2009.01.122](https://doi.org/10.1016/j.jnucmat.2009.01.122)

This is a PDF file of an unedited manuscript that has been accepted for publication. As a service to our customers we are providing this early version of the manuscript. The manuscript will undergo copyediting, typesetting, and review of the resulting proof before it is published in its final form. Please note that during the production process errors may be discovered which could affect the content, and all legal disclaimers that apply to the journal pertain.

MARFE stability and movement in an ELMy H-mode NSTX DischargeF. Kelly^{a*}, R. Maingi^b, R. Maqueda^c, J. Menard^a, S. Paul^a^a *Princeton Plasma Physics Laboratory, Princeton, NJ USA*^b *Oak Ridge National Laboratory, Oak Ridge, TN USA*^c *Nova Photonics, Princeton, NJ USA***Abstract**

The results of a comparison of Multifaceted Asymmetric Radiation From the Edge (MARFE) theory with experiment in the National Spherical Torus Experiment (NSTX) are presented. A variety of MARFE behavior was observed using a fast-framing camera. A basic MARFE theory was applied to NSTX Multi-Pulse Thomson scattering (MPTS) and charge-exchange recombination spectroscopy (CHERS) data. MARFE theory showed some limited agreement with experiment, but uncertainty in the separatrix location constrained the analysis. A method based on shifting iso- T_e flux surfaces was used to estimate the separatrix location. The movements of MARFEs in NSTX are interpreted to result from diamagnetic heat flux driven drifts relative to the background plasma velocity and imply slowing edge poloidal rotation and/or changing edge profiles before a large ELM.

PACS: 52.40.Hf, 52.55.Dy, 52.55.Hc, 52.70.Kz

JNM keywords: E0500 Experimental techniques, T0100 Theory and Modeling

PSI-18 keywords: NSTX, MARFE, ELM, Particle drifts, Visible imaging

*Corresponding author address: MS 34, PPPL, P.O. Box 451, Princeton, NJ 08543

*Corresponding author e-mail address: fkelly@pppl.gov

1. Introduction

Density limits in L-mode operation are usually associated with MARFEs [1], while ELMs are associated with H-mode operation. The NSTX is apparently unique among toroidal confinement devices in that MARFEs and ELMs can coexist within the same H-mode discharge [2] without the MARFE limiting performance or causing an H-L transition. In this paper, we present the results of an analysis of MARFE stability and movement in NSTX. The MARFE, which naturally occurs on the last closed flux surface (LCFS) of limiter tokamaks and the separatrix of diverted tokamaks, provides a possible means to explore edge transport processes and infer edge parameter changes. A method based on shifting iso- T_e flux surfaces in ψ_N space was used to locate the separatrix.

NSTX operates using up to 7 MW of neutral beam injection at low aspect ratio with $R = 0.85$ m and $a = 0.65$ m ($R/a \approx 1.3$), elongations up to 2.8, plasma currents up to 1.5 MA, $B_T = 0.3$ to 0.55 T and triangularities up to 0.8 [3]. Plasma facing components consist of a combination of graphite and carbon fiber composite tiles. The dominant impurity is carbon. The D-fueled NSTX discharge (117125) modeled in this paper was conducted with plasma current $I_p = 0.9$ MA and on-axis toroidal field $B_t = 0.45$ T, in a near double null discharge shape (favoring the lower X-point) with elongation $\epsilon \sim 2.4$, triangularity $\delta \sim 0.7$, and the ion grad-B drift toward the lower X-point.

2. Experimental observations and measurements

Rapidly evolving MARFE and ELM structures were observed in NSTX using a Phantom 7.1 fast-framing digital camera [2]. A wide-angle, fish eye elevation view of the center column together with upper and lower divertor regions were obtained for NSTX shot 117125 with a D_α-line bandpass filter. Before a MARFE forms, a highly-radiating,

poloidally and toroidally localized region of cold, dense plasma (plasmoid) is typically seen to spiral helically around the center column, approximately following the magnetic field pitch (Fig. 4a of Ref. 2). This plasmoid can be the result of small ELM activity in which heat is transported from the ELM filaments to a ring MARFE that encompasses the center stack. The heat flux partially burns through the ring MARFE and the remnant plasmoid moves upward from the lower divertor following the local magnetic field line. The motion of the plasmoid stagnates, typically above the midplane, after the ELM. The ring MARFE reforms and moves downward towards the lower divertor. Several cycles of this MARFE/ELM interaction are shown in Fig. 1. The downward velocity of the ring MARFE is calculated from the slope at the middle of the streak image relative to the 2 m center stack and is seen to be slowing from 1.77 km/s at 658 ms, to 1.54 km/s at 660 ms, to 1.49 km/s at 661.5 ms, to 1.46 km/s at 663 ms. By 665 ms the MARFE has intensified and its downward velocity has slowed to 0.94 km/s. Just before a Type I ELM occurs, the MARFE changes direction and is completely burned. The variations in MARFE velocity and intensity are presumably due to changing edge parameters. Plasmoids are also observed to originate spontaneously from the divertor region or near the center stack gas puff and evolve into MARFEs.

The kinetic profile diagnostics used to measure the edge parameters consisted of the 30 channel MPTS and 51 channel CHERS systems. Since the plasma profiles are dynamically evolving and the CHERS measurement is averaged over 7.11 ms [4], the MARFE stability analysis is restricted to times where the MPTS time and the middle of the CHERS time average interval nearly coincide due to the unreliability of the carbon fraction at other times. Even with this restriction, the carbon fraction, $f_C = n_C/n_e$, estimated from the CHERS C^{6+} density and MPTS electron density sometimes appears to be rather large at the

separatrix, e.g. at 627 ms. This is probably due to the different spatial resolutions of the CHERS and MPTS systems in the steep n_e gradient region.

The spatial resolution of the MPTS measurement is not quite sufficient to resolve the electron temperature and density in the NSTX plasma edge where steep gradients exist in H-mode. We depend on spline fitting to obtain estimates from the MPTS data. A serious complication is that the equilibrium codes EFIT and LRDFIT [5] do not accurately determine the location of the low field side (LFS) separatrix. We assume the high field side (HFS) flux surfaces are more accurately determined by the equilibrium code (due to the order of magnitude smaller Δ_N error of the innermost MPTS channel and the close proximity of the flux loops and B-field measurement coils on the HFS) and adjust the MPTS and CHERS profiles by shifting the LFS T_e data points in Δ_N space until the fitted profile overlays the innermost T_e data point from the HFS. This innermost MPTS channel has high radial resolution due to the laser beam being tangent to the flux surface at this point [6]. $T_{e,HFS}$ from this innermost MPTS channel is unusable if magnetic islands or MARFES are nearby and one must either align the LFS and HFS profiles visually or use the less accurate 2nd innermost MPTS channel.

The observations and measurements using the procedures described above using equilibrium reconstructions are summarized in Table 1. 1.4 ms is added to the reported CHERS time to locate the center of the integration interval [4]. Since the CHERS data didn't reach the estimated separatrix in about 1/3 of the samples, the maximum carbon fraction between the 0.90 and 1.00 poloidal flux surfaces was used. The uncertainties in the data are large. The flux surface shifting method can fail apparently due to a degraded

equilibrium calculation, e.g. near large ELMs at 527 and 543 ms or from 3D perturbations at 410 and 810 ms or for unknown reasons at 593 ms. At 643, 660, 677 and 710 ms, MARFEs affected the innermost MPTS channel and the LFS and HFS T_e profiles were aligned visually. Fig. 2 shows examples of fast-camera images of the MARFE conditions referred to in Table 1, beginning with ‘no MARFE’, ‘MARFE onset’, and other conditions where a MARFE exists. ‘MARFE onset’ means visible plasmoids leading to MARFE formation. ‘Stable at top’ means a MARFE has moved up the center stack, stopped and intensified. Note the very bright D₊ light from the lower divertor for case (c) as the MARFE moves up. A ms before, during a Type I ELM, the D₊ light was even brighter and a cloud of ablated material appeared around the lower divertor.

3. MARFE stability theory

MARFEs were first reported in Alcator-C and attributed to a radiative thermal instability in the parallel energy balance by Lipschultz [7]. Mahdavi [8] and Maingi and Mahdavi [9] incorporated the non-equilibrium radiation effect of neutrals in a uniform edge distribution to obtain

$$n_{marfe} = \frac{(\kappa_0 / Z_{eff}) T^{1/2} / (qR)^2}{\sqrt{-\sum_z f_z \frac{\partial}{\partial T} \left(\frac{L_z(T, f_0)}{T^2} \right)}} \quad (1)$$

the MARFE density limit, where $\kappa_{||} = (\kappa_0 / Z_{eff}) T^{5/2}$ is the Spitzer parallel conductivity,

$f_z = n_z/n_e$ is the impurity fraction and $f_0 = n_0/n_e$ is the neutral fraction. Defining the

MARFE Index, $MI = n_e/n_{marfe}$, the calculation of MARFE stability for NSTX discharge

117125 by Eq. (1) is shown in Fig. 3 using the Thomson and CHERS data in Table 1 and

$f_0 = 10^{-3}$ was estimated near the separatrix of this shot with the XGC0 code [10]. Figure 3 shows rough agreement between Eq. (1) and NSTX experiment, except at high density.

4. MARFE movement

Chankin [11] found that the growth rate of the MARFE instability is unaffected by the poloidal E_B drift. Chankin's analysis found that the only consequence of poloidal E_B rotation was that the poloidal rotation of the MARFE was at the same velocity as the background plasma. In H-mode plasmas, the radial electric field just inside the separatrix is negative. Thus, in NSTX shot 117125 the movement of the MARFE should be directed downward, however, at 377 ms the MARFE was observed moving upward. Another possible explanation is offered by Tokar [12]. The MARFE moves because one of the MARFE borders is cooled and the other heated by drift diamagnetic heat flows, due to their pressure dependence. Here, we observe that the motion of the MARFE due to diamagnetic heat flows will be relative to the velocity of the background plasma.

We use non-stationary equations for heat transport taking into account heat flows both across and along magnetic surfaces. Due to the Shafranov shift of magnetic flux surfaces, the temperature and density gradients are largest at the LFS of the discharge. These gradients drive instabilities which cause the conductive heat flux density through the edge boundary, q_b , to be poloidally asymmetric. We assume the θ dependence of q_b to be of the form $q_b = \bar{q}_b(1 - \beta \cos \theta)$ where $\bar{q}_b = Q_b / A_p$, Q_b is the conductive power transported to the periphery, A_p is the area of the peripheral magnetic surface, β is the heat flux asymmetry factor and $\beta = 0$ at the HFS midplane. We assume that the ratio of the average conductive heat flux on the LFS to the average over the whole surface is $\bar{q}_{LFS} / \bar{q}_b = 0.75$, thus $\beta = \pi / 4$.

We use LRDFIT calculated values of A_p , neutral beam and ohmic heating powers and measured values of the radiative power loss together with an assumed conductive fraction of 0.5 to estimate Q_b and q_b . We assume the radial thermal diffusivity at the separatrix, χ_r , to be $50 \text{ m}^2/\text{s}$. The radial thermal conductivity was calculated from $\kappa_r = n_e \chi_r$.

Defining $\alpha_{vT} = \nabla_r T_i / \nabla_r T_e$, $\alpha_T = T_i / T_e$ and taking $\frac{\partial T}{\partial r} = -\frac{q_b}{\kappa_r}$, we may write

$$q_{d,\perp} = \frac{5}{2} \frac{P}{eB} \frac{q_b}{\kappa_\perp} (1 - \alpha_{vT} \alpha_T). \text{ Taking the terms describing the dependencies of the pressure on}$$

t and ϑ , and assuming the other terms constant, the heat equation becomes:

$$\frac{3}{2} \frac{\partial P}{\partial t} + \frac{5}{2} (1 - \alpha_{vT} \alpha_T) \frac{q_b}{eB\kappa_r a} \frac{\partial P}{\partial \vartheta} = C \quad (2)$$

where $P = n(T_i + T_e)$ and a is the minor radius. Perturbations of P in the form $\tilde{P} \propto \exp(V_{\theta d} t - a \vartheta)$ yield an estimate of the poloidal diamagnetic drift velocity

$$V_{\theta d} = \frac{5}{3} \frac{q_b}{eB\kappa_r} (1 - \alpha_{vT} \alpha_T) \quad (3)$$

Using LFS Thomson measurements of n_e and T_e and CHERS measurements of T_i , we estimate for shot 117125 at 377 ms $\alpha_{vT} = 3.9$, $\alpha_T = 9.4$ and $V_{\theta d} = 1.0 \text{ km/s}$ upward. At 660 ms, we estimate $\alpha_{vT} = 0.85$, $\alpha_T = 8.2$ and $V_{\theta d} = 3.6 \text{ km/s}$ upward. From the fast-framing camera images the experimental poloidal velocity of the MARFE is estimated to be 1.88 km/s upward at 377 ms and 1.54 km/s downward at 660 ms. If the total poloidal MARFE velocity is the diamagnetic heat flux driven drift relative to the background plasma velocity, then the E_{θ} drift is 1.7 km/s downward with $E_r = -3.3 \text{ kV/m}$ at 377 ms and $E_{\theta} = 2.6 \text{ km/s}$

downward with $E_r = -4.6$ kV/m at 660 ms. Values of the E_r in this range during H-mode were measured by Biewer [13] in a similar NSTX shot 110077. The calculation illustrates that reasonable assumptions lead to MARFE velocities that are in the right direction and within an order of magnitude of experimental measurements.

5. Discussion and Conclusions

In order to perform analysis of the edge in a diverted tokamak, one must first locate the separatrix and then obtain reasonable estimates of edge parameters. The separatrix location was estimated by shifting the LFS T_e profile to overlay a HFS T_e point considered to be accurate. In 12 of 14 cases, values of T_e at the separatrix at MARFE onset or during MARFEs were in the range of 31 to 41 eV, which is similar to the ranges observed in TEXTOR at MARFE onset with a He beam diagnostic with different data processing [14-16]. The separatrix densities in NSTX, however, are higher. The MARFE density limit predicted by basic MARFE theory, roughly agrees with NSTX experimental observation, except in the highest density phase. We found that if the poloidal movement of the MARFE is the diamagnetic heat flux drift relative to the background plasma velocity, (e.g. E_B drift), then MARFE movement in NSTX may be explained with an $E_r \approx -4$ kV/m. This model implies that before the large ELM in Fig. 1 that the edge poloidal rotation may be slowing and/or the edge profiles are changing.

Acknowledgements

Research sponsored in part by U.S. D.o.E. contracts DE-FG02-04ER54767, DE-AC02-76CH03073 and DE-AC05-00OR22725.

References

- [1] B. Lipschultz, J. Nucl. Mater. 145-147 (1987) 15.
- [2] R.J. Maqueda, R. Maingi, K. Tritz, et al., J. Nucl. Mater. 363-365 (2007) 1000.
- [3] J.E. Menard, M.G. Bell, R.E. Bell, et al., Nucl. Fusion 47 (2007) S645.
- [4] R.E. Bell (private communication, 2008)
- [5] J.E. Menard (private communication, 2007) The LRDFIT Grad-Shafranov equilibrium reconstruction code used in '04' mode incorporates constraints from magnetics and in the core T_e iso-surfaces.
- [6] B. LeBlanc (private communication, 2008)
- [7] B. Lipschultz, B. LaBombard, E.S. Marmor, et al., Nucl. Fusion 24 (1984) 977.
- [8] M.A. Mahdavi, et al., in *Proc. 24th European Conf. Controlled Fusion and Plasma Physics*, Berchtesgaden, Germany, 1997, Vol. 21A, p. 1113, (European Physical Society, 1997).
- [9] R. Maingi and M.A. Mahdavi, Fusion Sci. and Technol. 48 (2005) 1117.
- [10] C.S. Chang, S. Ku and H. Weitzner, Phys. Plasma 11 (2004) 2649.
- [11] A.V. Chankin, Phys. Plasma 11 (2004) 1484.
- [12] M. Z. Tokar, Contrib. Plasma Phys. 32 (1992) 341.
- [13] Biewer, et al., Rev. Sci. Inst. 75 (2004) 650.
- [14] J. Rapp, H.R. Koslowski, M. Lehnen, et al., in : Proc. 26th Conf. Plasma Physics Control. Fusion, Maastricht, Europhys. Conf. Abstr., vol. 23J, 1999, p. 665.
- [15] J. Rapp, H.R. Koslowski, M. Lehnen, et al., J. Nucl. Mater. 290-293 (2001) 1148.
- [16] F.A. Kelly, W.M. Stacey, J. Rapp and M. Brix, Phys. Plasmas 8 (2001) 3382.

Figure captions

Table 1: MARFE observations for NSTX discharge 117125 at the Thomson Scattering times and the data used in the MARFE stability calculation if t_{TS} and $t_{CHERS} + 1.4$ ms coincide.

Fig. 1: MARFE/ELM cycles in NSTX discharge 117125: (a) “streak” image showing the plasmoid spiral upward, stagnate, reform a MARFE which moves downward until an ELM partially burns through the MARFE leaving a plasmoid as a remnant to begin a new cycle and (b) the D_{α} light signal from the lower divertor.

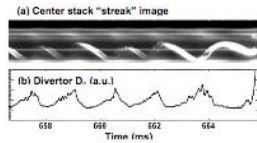


Fig. 2: Conditions observed in NSTX discharge 117125: (a) no MARFE, $t = 0.326662$ s; (b) MARFE onset, $t = 0.726662$ s; (c) move up, $t = 0.376685$ s; (d) stagnation, $t = 0.493322$ s; (e) move down, $t = 0.660002$ s; (f) burn, $t = 0.626662$ s; (g) stable at top, $t = 0.676685$ s. The center image is nearest the TS time given, the left image -72.5 μ s earlier and the right image $+72.5$ μ s later.

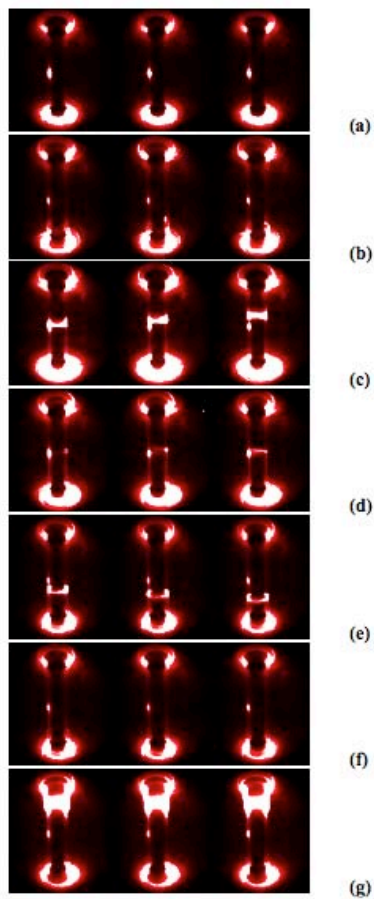


Fig. 3: MARFE Index plotted at the sample times of Table 1 when t_{TS} and $t_{CHERS} + 1.4$ ms coincide.

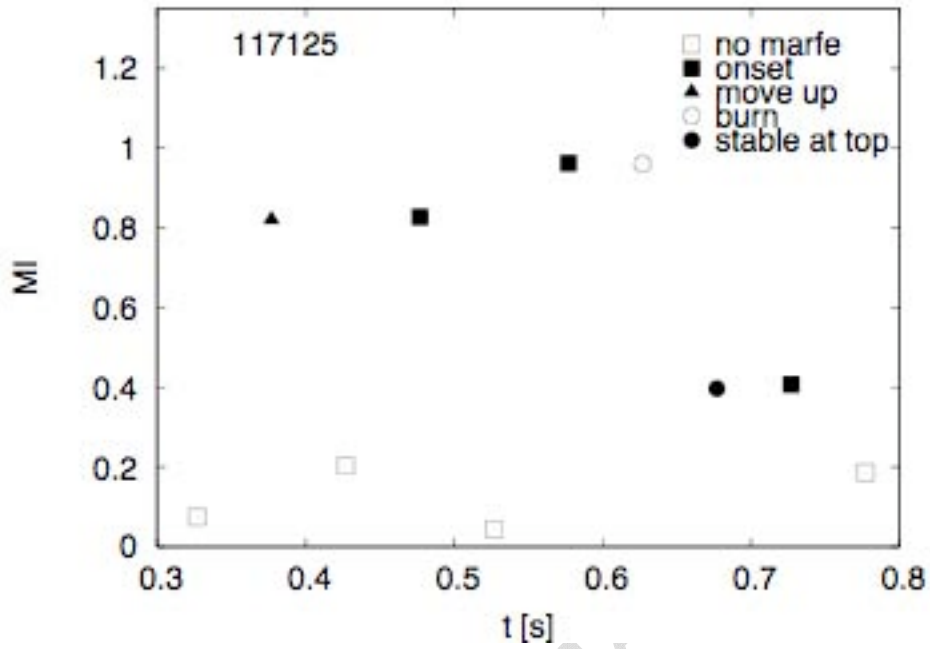


Table 1:

TS time [s]	Condition	CHERS time + 1.4 ms	T_e [eV]	n_e [m^{-3}]	f_C [%]
0.326662	no marfe	0.32665	93	2.5E19	7.2
0.343345	no marfe	0.34665	101	2.9E19	
0.359992	no marfe	0.35665	71	2.6E19	
0.376685	upward move	0.37665	34	2.2E19	6.4
0.393332	no marfe	0.39665	99	2.4E19	
0.410015	no marfe	0.40665	94	1.9E19	
0.426662	no marfe	0.42665	51	1.8E19	5.2
0.443345	no marfe	0.44665	64	2.2E19	
0.459992	no marfe	0.45665	53	2.1E19	
0.476685	onset	0.47665	38	3.0E19	6.2
0.493322	stagnation	0.49665	34	2.1E19	
0.510025	stagnation	0.50665	33	1.9E19	
0.526662	no marfe	0.52665	147	3.4E19	4.9
0.543345	onset	0.54665	35	1.4E19	
0.559992	no marfe	0.55665	53	2.2E19	
0.576685	onset	0.57665	31	1.9E19	6.8
0.593332	onset	0.59665	58	2.6E19	
0.610025	no marfe	0.60665	41	1.9E19	
0.626662	burn	0.62665	34	1.8E19	10.7
0.643355	stagnation	0.64665	35	1.9E19	
0.660002	move down	0.65665	32	1.5E19	
0.676685	stable at top	0.67665	41	2.2E19	4.5
0.693332	no marfe	0.69665	41	2.3E19	
0.710015	onset	0.70665	35	2.2E19	
0.726662	onset	0.72665	41	2.2E19	4.8
0.743355	no marfe	0.74665	50	1.6E19	
0.759992	no marfe	0.75665	68	2.8E19	
0.776685	no marfe	0.77665	61	2.5E19	5.9
0.793332	no marfe	0.79665	75	2.5E19	
0.810015	stagnation	0.80665	60	2.6E19	

The Princeton Plasma Physics Laboratory is operated
by Princeton University under contract
with the U.S. Department of Energy.

Information Services
Princeton Plasma Physics Laboratory
P.O. Box 451
Princeton, NJ 08543

Phone: 609-243-2750
Fax: 609-243-2751
e-mail: pppl_info@pppl.gov
Internet Address: <http://www.pppl.gov>